Biochemistry

Volume 15, Number 1 January 13, 1976

Investigation of Quercetin Binding Sites on Chloroplast Coupling Factor 1†

Lewis C. Cantley, Jr.,‡ and Gordon G. Hammes*

ABSTRACT: The quercetin binding sites on spinach chloroplast coupling factor 1 (CF_1) have been investigated using direct and competitive binding, stopped-flow, temperature-jump, and fluorescence resonance energy transfer measurements. It was found that 8-anilino-1-naphthalenesulfonic acid (ANS) competes with quercetin binding at two sites on the solubilized enzyme which are distinct from the two tight nucleotide binding sites and the 7-chloro-4-nitrobenzo-2-oxa-1,3-diazole (NBD-Cl) reactive site. The bimolecular association of quercetin with CF_1 is too fast to measure directly and is followed by two slower conformational changes. The distances from the tight nucleotide sites to the quercetin-ANS sites were estimated as 40–48 Å by fluorescence resonance energy transfer using 1,N^6-ethenoadenosine diphosphate and 1,N^6-ethenoadenylyl imidodiphosphate as donors and quercetin as the acceptor. The distance from the quercetin-ANS site to the NBD-Cl reactive site was found to be about 30 Å using ANS as a donor and NBD-Cl reacted with a tyrosine group on CF_1 as the energy acceptor. A model is proposed for the relative location of these sites on CF_1.

Purified preparations of coupling factor (CF_1)[1] solubilized from spinach chloroplasts contain five different subunits (Lien et al., 1972), α, β, γ, δ, and ϵ, with respective molecular weights of 59000, 56000, 37000, 17500, and 13000. The total molecular weight is 325000 (Farron, 1970), and the solubilized CF_1 appears to be spherical in shape with an approximate diameter of 100 Å (Howell and Moudrianakis, 1967). The Ca^{2+}-ATPase activity is located on the α-β subunits, and this activity can be abolished by modification with NBD-Cl of a tyrosine located on a β subunit (Deters et al., 1975). Binding and steady-state kinetic experiments (Cantley and Hammes, 1975a) have indicated the presence of two tight binding sites on solubilized CF_1 which bind ADP, ϵADP, AMP-PNP, and ϵAMP-PNP and a single active site for ATP hydrolysis on the heat-activated enzyme. The tight nucleotide sites appear to act as allosteric conformational switches of the Ca^{2+}-ATPase activity. Fluorescence energy transfer measurements have shown that the tight nucleotide sites are approximately 40 Å away from the NBD-Cl reactive site (Cantley and Hammes, 1975b).

Quercetin has an inhibitory effect on the Ca^{2+}-ATPase activity of CF_1 (Deters et al., 1975) but appears to stimulate the photophosphorylation activity of extensively dialyzed chloroplasts (Lardy et al., 1964). Quercetin also inhibits the ATPase activity of the mitochondrial coupling factor, F_1, without affecting oxidative phosphorylation (Lang and Racker, 1974). In this work the quercetin binding sites on solubilized CF_1 are investigated using direct and competitive binding, stopped-flow, and temperature-jump measurements. ANS is found to compete with quercetin binding at two sites on CF_1. The distances from these sites to the tight nucleotide sites and to the NBD-Cl reactive site were measured by the method of fluorescence resonance transfer using the donor–acceptor pairs ϵADP–quercetin, ϵAMP-PNP–quercetin, and ANS–NBD-Tyr, and a model is proposed for the location of these sites on CF_1.

Experimental Section

Materials. The [^{3}H]ϵADP and [^{3}H]ϵAMP-PNP were prepared as previously described (Cantley and Hammes, 1975a). The quercetin was purchased from Eastman Chemical Co., the NBD-Cl from Pierce Chemical Co., the quinine sulfate from Aldrich Chemical Co., and the ANS from Sigma Chemical Co. All other chemicals were the best

† From the Department of Chemistry, Cornell University, Ithaca, New York 14853. *Received August 11, 1975.* This work was supported by a grant from the National Institutes of Health (GM 13292).

‡ National Science Foundation Fellow and National Institutes of Health Trainee (GM 00834).

[1] Abbreviations used are: CF_1, chloroplast coupling factor 1; F_1, mitochondrial coupling factor 1; NBD-Cl, 7-chloro-4-nitrobenzo-2-oxa-1,3-diazole; ϵADP, 1,N^6-ethenoadenosine diphosphate; AMP-PNP, adenylyl imidodiphosphate; ϵAMP-PNP, 1,N^6-ethenoadenylyl imidodiphosphate; ANS, 8-anilino-1-naphthalenesulfonate; NBD-Tyr-CF_1, NBD-Cl reacted with the phenolic oxygen of a tyrosine moiety on CF_1.

available commercial grades, and all solutions were prepared with deionized distilled water.

CF_1 and NBD-Tyr-CF_1 Preparations. CF_1 was prepared by known procedures (Lien and Racker, 1971). An extinction coefficient of 0.476 ml/(mg cm) (Cantley and Hammes, 1975a) at 280 nm in 0.1 *M* NaCl, 50 m*M* TrisCl, and 5 m*M* $CaCl_2$ (pH 8.0), 23°, was used to determine protein concentrations of CF_1 solutions free of exchangeable nucleotides. A molecular weight of 325000 (Farron, 1970) was used to determine the molar concentrations of enzyme. The NBD-Cl modified CF_1 in which the NBD moiety is attached to one or two tyrosine groups per mole of enzyme (NBD-Tyr-CF_1) was prepared as described elsewhere (Cantley and Hammes, 1975a), and an extinction coefficient of $10.7 \times 10^3\ M^{-1}\ cm^{-1}$ at 400 nm was used to determine the stoichiometry of NBD covalently bound to CF_1. The enzyme was passed through two Sephadex G-25 (medium) columns immediately before use to remove exchangeable nucleotides (Cantley and Hammes, 1975a).

Difference Spectra Measurements. Rectangular quartz tandem cells (Pyrocell Manufacturing Co.) having a 0.44-cm path length in each chamber were used to measure the difference spectrum resulting from the interaction of quercetin with solubilized CF_1. The difference spectrum was recorded on a Cary 14 recording spectrophotometer equipped with a 0–0.1-absorbance slide-wire. Difference spectrum titrations were done using a Zeiss spectrophotometer at constant slit width (cf. Anderson et al., 1968). The quercetin was dissolved in 95% ethanol (10 m*M*) and added to the enzyme in 0.1 *M* NaCl, 50 m*M* Tris-Cl, 5 m*M* $CaCl_2$, and 1 m*M* dithiothreitol (pH 8.0), 23°. The dithiothreitol was present to stabilize quercetin in a reduced state. The final ethanol concentration was less than 4%.

Steady-State Fluorescence Measurements. The steady-state fluorescence measurements were made with a Hitachi-Perkin-Elmer MPF-3 fluorescence spectrophotometer. The quantum yield of ANS bound to CF_1 in 0.1 *M* NaCl, 50 m*M* Tris-Cl, and 5 m*M* $CaCl_2$ (pH 8.0), 23°, was determined by a comparative method (Parker and Rees, 1966).

$$Q_1/Q_2 = (F_1/F_2)(A_2/A_1)/(1 - r_b/4) \qquad (1)$$

Equation 1 gives the ratio of quantum yields, Q_i, as a function of the area of the corrected emission spectrum, F_i, and the absorbance at the exciting wavelength, A_i, for two different fluorescing compounds. The factor $(1 - r_b/4)^{-1}$ is a correction for polarized emission (Shinitzky, 1972), and r_b is the anisotropy of bound ANS. Quinine sulfate in 0.1 *N* H_2SO_4 was used as a standard and was assumed to have an absolute quantum yield, Q_2, of 0.70 (Scott et al., 1970) at 23°. In order to calculate the absorbance of ANS bound to CF_1, A_1, it was necessary to determine the extinction coefficient and the concentration of ANS bound to CF_1. The concentration of ANS bound to CF_1 was calculated using the dissociation constants determined as described below, and the extinction coefficient, $6.17 \times 10^3\ M^{-1}\ cm^{-1}$ at 370 nm, was calculated from the difference spectrum of ANS with CF_1. The inner filter effect due to excess free ANS which does not fluoresce was corrected for by adding ANS to the quinine sulfate solution to a final absorbance equal to the free ANS absorbance in the enzyme solution. Both A_1 and A_2 were less than 0.05 at the exciting wavelength, 370 nm, and the area of the corrected emission spectrum was determined by cutting out and weighing the recorded spectrum.

In experiments measuring ANS binding to CF_1 or competitive binding of quercetin or 2,4-dinitrophenol with ANS by fluorescence intensity, it was necessary to correct for the inner filter effect due to the absorbance of these compounds at the exciting wavelength, 370 nm. This correction was calculated by a control experiment in which ANS was added to a quinine sulfate solution in 0.1 *N* H_2SO_4. The wavelengths (370-nm excitation, 470-nm emission), slits, and cuvette were identical in the control experiment, and the percent quenching of quinine sulfate fluorescence vs. ANS absorbance was plotted. From this curve, the inner filter effect due to nonfluorescing constituents could be calculated from their absorbance at 370 nm. The absorbance of bound ANS was always less than 0.05. Triangular (1 cm × 1 cm × 1.4 cm) and square micro (0.3 cm × 0.3 cm) cuvettes were used to minimize the inner filter effect.

The quantum yields of ϵADP and ϵAMP-PNP in the presence of quercetin were determined as follows. The change in fluorescence (320-nm excitation, 400-nm emission) with time of [^{3}H]ϵADP or [^{3}H]ϵAMP-PNP accompanying binding to CF_1 was measured (Cantley and Hammes, 1975a). After equilibrium was reached, the solutions were titrated with 5 m*M* quercetin in 95% ethanol and the fluorescence intensity was recorded. The free and total nucleotide concentrations were then immediately determined (in about 10 min) using the forced dialysis technique (Cantley and Hammes, 1973). As a control experiment, a large excess of unlabeled ADP (440 μM) was equilibrated with the enzyme before adding the labeled fluorescent nucleotide. The solution was then titrated with 5 m*M* quercetin as before, and the free and total labeled nucleotide concentrations were determined. The ADP prevented binding of the fluorescent nucleotide so that the inner filter effect of quercetin and the effect of the ethanol (<4% final concentration) on the fluorescence could be determined.

In addition to inner filter corrections, all fluorescence measurements were corrected for light scattering due to the protein and for dilution effects. The fluorescence polarization measurements were corrected for light scatterng, and a correction was made for unequal transmission of horizontally and vertically polarized light by the emission monochromator grating (Azumi and McGlynn, 1962).

Fluorescence Lifetime Measurements. Fluorescence lifetimes were measured with an ORTEC Model 9200 nanosecond fluorescence spectrophotometer (Matsumoto and Hammes, 1975). The excitation wavelength, 370 nm, was selected with a monochromator, and a 3-cavity interference filter centered at 470 nm (Ditric Optics, Inc.) was used to filter the emitted light. Triangular (1 cm × 1 cm × 1.4 cm) and square micro (0.3 cm × 0.3 cm) cuvettes were thermostated at 23°. A colloidal silica (Ludox HS-30) solution was used to determine the lamp spectrum. A scattering correction was made by photon counting an enzyme solution in the absence of ANS for an equal period of time and subtracting the counts from those of the sample. Data were analyzed on a PDP-11 computer with the deconvolution and convolution programs provided by ORTEC.

Kinetic Measurements. The equipment and procedures used for temperature-jump relaxation measurements have been described elsewhere (Faeder, 1970). The absorbance was monitored at the wavelength of maximum change in the difference spectrum for interaction of quercetin with CF_1, 410 nm. The temperature was jumped 7.5° to a final temperature of 23°, and the solution was buffered at pH 8.0 in 0.1 *M* NaCl, 50 m*M* sodium phosphate, and 1 m*M* dithiothreitol. The kinetic information was transferred directly on-line to a PDP-11 digital computer by a Biomation

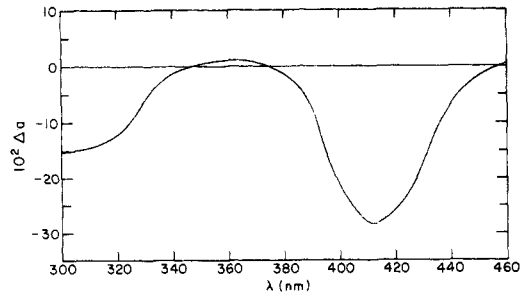

FIGURE 1: A typical difference spectrum for the interaction of quercetin (193 μM) with CF_1 (7.62 μM) in 0.1 M NaCl, 50 mM Tris-chloride, 5 mM $CaCl_2$, and 1 mM dithiothreitol (pH 8.0). The cell path length was 0.44 cm.

Model 802 transient recorder. The relaxation times and amplitudes were then calculated by means of single and double exponential least-squares programs. At least four kinetic measurements were made on each reaction mixture, and the data were averaged to enhance the signal to noise ratio (cf. Hilborn et al., 1973; Hilborn, 1972 for a detailed description of the data collection and analysis system).

Stopped-flow relaxation measurements were made with a Durrum-Gibson D-108 stopped-flow spectrophotometer. The quercetin and CF_1 were in 0.1 M NaCl, 50 mM sodium phosphate, and 1 mM dithiothreitol (pH 8.0), 23°. Equal volumes of the two reagent solutions were mixed, and the absorbance was monitored at 410 nm.

Results

The stoichiometry and affinity of quercetin binding to CF_1 were determined by difference spectrum titrations monitored at 410 nm. Figure 1 is a difference spectrum of the CF_1-quercetin interaction in 0.1 M NaCl, 50 mM Tris-Cl, 5 mM $CaCl_2$, and 1 mM dithiothreitol (pH 8.0), 23°. A general decrease in quercetin absorbance accompanies binding with a maximum change at 410 nm. (Quercetin has a maximum extinction coefficient of 16.1×10^3 M^{-1} cm^{-1} at 385 nm in this buffer.) In one set of titrations, the total quercetin concentration was held constant and the enzyme concentration was varied in order to estimate the difference extinction coefficient when all the quercetin is bound. In another set of titrations, the enzyme concentration was held constant and the quercetin concentration varied. The accumulated data were then analyzed by a least-squares iterative technique using eq 2 which assumes two types of noninteracting sites with equal difference extinction coefficients. The n_i are the number of sites of type i per mole of enzyme with intrinsic dissociation constants K_i, Δa is the measured difference in absorbance at 410 nm, $\Delta\epsilon$ is the difference extinction coefficient at 410 nm, (E_0) is the total enzyme concentration, and (L_0) is the total quercetin concentration. Whole number values were assigned to n_1 and n_2 and the parameters $\Delta\epsilon$, K_1, and K_2 were allowed to vary. The best fit to the data was attained with $n_1 = 2$, $n_2 = 2$, $K_1 = 19.5$ μM, $K_2 = 94.5$ μM, and $\Delta\epsilon = 4.43 \times 10^3$ M^{-1} cm^{-1}. The least-squares fit to the data is shown in Figure 2. The data did not exclude the possibility that $n_1 = 3$ and $n_2 = 1$ with $K_1 = 30.5$ μM, $K_2 = 278$ μM, and $\Delta\epsilon = 4.60 \times 10^3$ M^{-1} cm^{-1} but all other values for n_1 and n_2 gave poor fits to the data. Equation 2 is the simplest which adequately fits the data.

$$\Delta a = \frac{n_1(E_0)\Delta\epsilon(L_f)}{K_1 + (L_f)} + \frac{n_2(E_0)\Delta\epsilon(L_f)}{K_2 + (L_f)}$$
$$(L_f) = (L_0) - \Delta a/\Delta\epsilon \qquad (2)$$

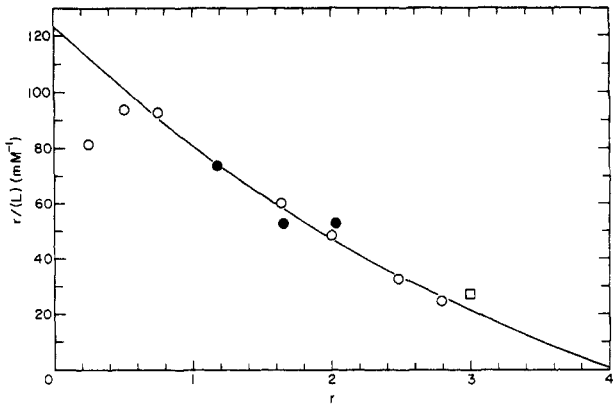

FIGURE 2: A plot of $r/(L)$ vs. r, where r is the number of moles of quercetin bound per mole of CF_1 and (L) is the concentration of free quercetin. The data were obtained by difference spectrum titrations (○) 29 μM CF_1 and 19.9–192 μM quercetin concentrations, (●) 49.5 μM quercetin and 5.56–28.8 μM CF_1 concentrations; and by forced dialysis (□) 192 μM quercetin and 28 μM CF_1. The buffer contained 0.1 M NaCl, 50 mM Tris-chloride, 5 mM $CaCl_2$, and 1 mM dithiothreitol (pH 8.0), and the free ligand concentration in the difference spectrum titrations was determined from an iterative least-squares fit of the data to eq 2.

The assumption of equal difference extinction coefficients for multiple sites is not always valid, but a more direct binding measurement such as equilibrium dialysis is difficult since the quercetin is not available in a radioactive form and shows a high affinity for dialysis tubing and all Diaflow membranes tested. The extent of quercetin binding to CF_1 at high enzyme and quercetin concentrations was estimated using the forced dialysis technique (Cantley and Hammes, 1973) under conditions where the free quercetin concentration could be measured by its absorbance at 485 nm. Diaflow XM-50 membranes were used and a correction was made for quercetin binding to the membrane (≈10%). As shown in Figure 2, the forced dialysis experiment result agrees well with the results obtained from the difference spectrum titration. A forced dialysis measurement was also made to estimate quercetin binding to the NBD-Cl modified enzyme. This enzyme bound quercetin with a stoichiometry similar to the native enzyme indicating that the NBD-Cl modification does not alter appreciably the quercetin binding to CF_1.

The binding of ANS to CF_1 in 0.1 M NaCl, 50 mM Tris-Cl, and 5 mM $CaCl_2$ (pH 8.0), 23°, was monitored by the large enhancement of ANS fluorescence (370-nm excitation, 470-nm emission) accompanying association with the enzyme. The fluorescence increment per mole of ANS bound was measured by titrating a fixed concentration of ANS (25.6 μM) with CF_1. The data were plotted as the reciprocal fluorescence vs. the reciprocal enzyme concentration, and the fluorescence at infinite protein concentration was calculated from a linear least-squares analysis of the data (Figure 3A). The ANS concentration was well below the dissociation constant so the approximation that the total enzyme equals the free enzyme is valid. The enzyme was then titrated with ANS using the same instrumental settings and use was made of the fluorescence increment to calculate the bound and free ANS. Both fluorescence titrations were corrected for inner filter effects and dilution effects (see the Experimental Section). The results are presented in Figure 3B as a plot of $r/(ANS)$ vs. r. Here r is the number of moles of ANS bound per mole of CF_1, and (ANS) is the free ANS concentration. The data were fit by

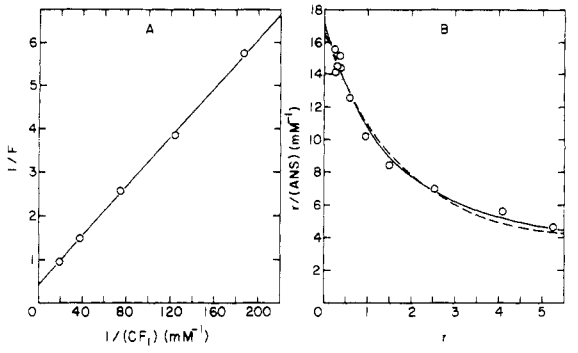

FIGURE 3: (A) A plot of $1/F$ vs. $1/(CF_1)$ where F is the fluorescence of ANS (370 excitation; 470 emission), and (CF_1) is the total enzyme concentration. The ANS concentration was constant at 25.6 μM. The line represents a linear least-squares fit to the data. (B) A plot of $r/(ANS)$ vs. r where r is the number of moles of ANS bound per mole of CF_1, and (ANS) is the free ligand concentration. The value of r was determined using the ANS fluorescence increment extrapolated to infinite protein concentration in Figure 3A and the curves were calculated from eq 3 and the sets of parameters $n_1' = 1$, $K_1' = 83$ μM, $n_2' = 15$, $K_2' = 2.93$ mM (—) and $n_1' = 2$, $K_1' = 150$ μM, $n_2' = 30$, $K_2' = 10$ mM (- - - -). All measurements were carried out in 0.1 M NaCl, 50 mM Tris-chloride, and 5 mM $CaCl_2$ (pH 8.0).

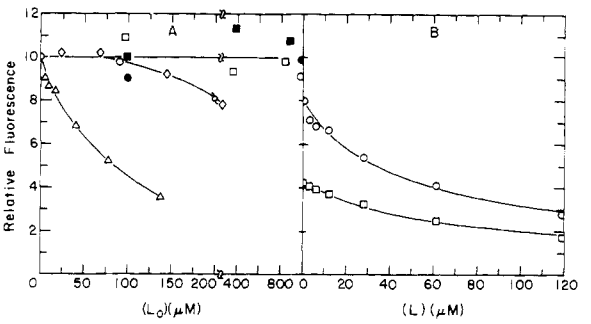

FIGURE 4: (A) The relative fluorescence of ANS interacting with CF_1 in the presence of the following ligands at varying concentrations: (○) ATP, (●) GTP, (□) ADP, (◇) 2,4-dinitrophenol, and (△) quercetin. The ANS concentration was 10–30 μM, the CF_1 concentration was 2.4–10 μM, and (L_0) is the total ligand concentration. (B) The relative fluorescence of ANS interacting with CF_1 (○) and NBD-Tyr-CF_1 (□) vs. the concentration of free quercetin (L). In both titrations, the enzyme concentration was 10.1 μM and the ANS concentration was 24.4 μM. The curves were calculated using eq 4, 5, and 6 as described in the text. All measurements were carried out in 0.1 M NaCl, 50 mM Tris-chloride, 5 mM $CaCl_2$, and 1 mM dithiothreitol (pH 8.0).

a non-linear least-squares analysis to eq 3 which assumes two types of noninteracting sites. The n_i' are the number of each type of site per mole of enzyme and the K_i' are the respective intrinsic dissociation constants. Whole number values were assigned to n_1' and the other three parameters were allowed to vary. As illustrated in Figure 3B, good fits were attained using the sets of parameters $n_1' = 1$, $K_1' = 83$ μM, $n_2' = 15$, $K_2' = 2.93$ mM or $n_1' = 2$, $K_1' = 150$ μM, $n_2' = 30$, $K_2' = 10$ mM. All other values of n_1' gave poor fits to the data. The procedure used to determine the fluorescence increment only gives the fluorescence increment of the tight sites; therefore the number of weak sites is poorly determined.

$$\frac{r}{(\mathrm{ANS})} = \frac{n_1'}{K_1' + (\mathrm{ANS})} + \frac{n_2'}{K_2' + (\mathrm{ANS})} \qquad (3)$$

A series of competitive binding experiments was conducted to determine if the binding of ANS to the tight sites is influenced by nucleotides and effectors of CF_1. The ANS concentration was less than 25 μM to ensure that most of the fluorescence was due to ANS bound to the tight sites. The fluorescence (370-nm excitation, 470-nm emission) was then monitored while titrating the enzyme plus ANS solution with various effectors including ATP, GTP, ADP, phosphate, 2,4-dinitrophenol, and quercetin. The fluorescence intensity was corrected for inner filter and dilution effects as described in the Experimental Section. The data presented in Figure 4A show that while millimolar concentrations of nucleotides or phosphates have no effect on the ANS fluorescence, quercetin decreases the fluorescence at low concentrations ($\approx$10 μM). The 2,4-dinitrophenol only slightly affects the ANS fluorescence. At high dinitrophenol or quercetin concentrations the inner filter effect became too large to allow accurate measurements. In view of the similar structures of quercetin and ANS (Figure 5), it seems likely that they are competing for the same sites on the enzyme.

A competitive binding model, described by eq 4, was devised for the displacement of ANS by quercetin assuming, as is suggested by the independent binding measurements, that two sites of CF_1 bind both ANS and quercetin. In eq 4,

$$\frac{r}{(\mathrm{L})} = \frac{2}{(\mathrm{L}) + K_1[1 + (\mathrm{ANS})/K_1']} + \frac{2}{(\mathrm{L}) + K_2} \qquad (4)$$

r is the number of moles of quercetin bound per mole of CF_1, (L) is the free quercetin concentration, (ANS) is the free ANS concentration, K_1 is the quercetin dissociation constant at the competitive sites, K_2 is the quercetin dissociation constant at the weak sites, and K_1' is the ANS dissociation constant at the competitive site. The analogous equation for ANS binding is eq 5:

$$F/C = r = \frac{2(\mathrm{ANS})}{(\mathrm{ANS}) + K_1'[1 + (\mathrm{L})/K_1]} + \frac{30(\mathrm{ANS})}{(\mathrm{ANS}) + K_2'} \qquad (5)$$

where F is the fluorescence intensity of bound ANS, C is the fluorescence increment, r is the number of moles of ANS bound per mole of CF_1, r_1 and r_2 are the number of moles bound to the tight and weak sites, and K_2' is the dissociation constant for ANS at the weak sites. Using an iterative technique to determine the free ANS and quercetin concentrations from eq 4 and 5, the decrease in ANS fluorescence caused by added quercetin was fit to eq 5 by a nonlinear least-squares analysis. The dissociation constants, $K_1' = 150$ μM, $K_2 = 94.5$ μM, and $K_2' = 10$ mM were taken from the independent binding measurements, C was determined in the absence of quercetin, and K_1 was determined to be 34 μM ($\pm$20%) from the least-squares fit. Allowing n_2' (for ANS) and K_2' to vary had little effect on the fit to K_1. The least-squares fit to the data is presented in Figure 4B.

The emission spectrum of ANS overlaps the absorption spectrum of NBD-Tyr-CF_1 sufficiently (Figure 6) so that resonance energy transfer can occur if the bound ANS is sufficiently close to the bound NBD. The change in the steady-state fluorescence increment for ANS binding to the NBD modified enzyme (1.0 mol/mol) was determined in an analogous competitive binding experiment with identical concentrations of ANS, enzyme, and quercetin. The data were fit to eq 6 by a least-squares analysis using the values of r_1, r_2, and C determined for the native enzyme and the fractional ANS fluorescence quantum yields at the tight and weak sites of the NBD modified enzyme, (Q_1/Q) and

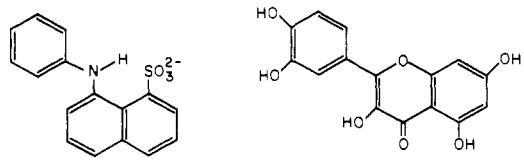

FIGURE 5: The structures of ANS and quercetin.

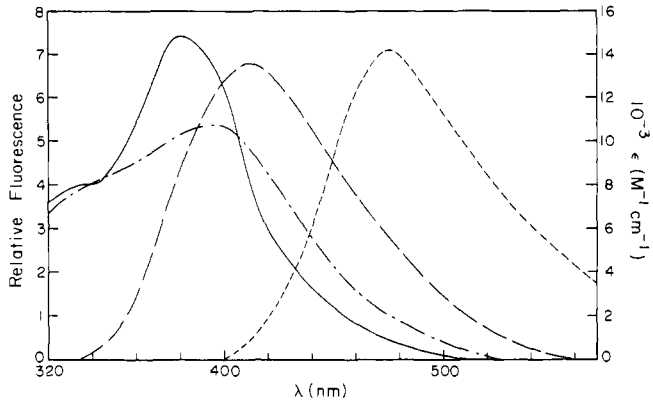

FIGURE 6: Overlap of the corrected fluorescence emission of ϵADP excited at 320 nm (— —) with the extinction coefficient (ϵ) of quercetin (—) bound to CF_1 and of the corrected fluorescence emission of ANS bound to CF_1 excited at 370 nm (- - - -) with the difference extinction coefficient (ϵ) of NBD-Tyr (— - —). The spectra were measured in 0.1 *M* NaCl, 50 m*M* Tris-chloride, 5 m*M* $CaCl_2$ (pH 8.0), and 1 m*M* dithiothreitol was present when measuring the quercetin spectrum.

(Q_2/Q), were determined to be 0.45 and 0.77, respectively. The least-squares fit to the data is presented in Figure 4B.

$$F/C = r_1(Q_1/Q) + r_2(Q_2/Q) \qquad (6)$$

The efficiency of energy transfer, E, is given by

$$E = 1 - Q_{D\rightarrow A}/Q_D = 1 - \tau_{D\rightarrow A}/\tau_D \qquad (7)$$

where $Q_{D\rightarrow A}$ and $\tau_{D\rightarrow A}$ are the quantum yield and fluorescence lifetime of the donor in the presence of the acceptor, and Q_D and τ_D are the quantum yield and fluorescence lifetime of the donor in the absence of transfer. The quantum yield of ANS bound to native CF_1 is 0.78. The fractional fluorescence yield of ANS bound to the tight sites in the presence of NBD-Tyr is 0.45 as determined above so that the energy transfer efficiency is 0.55. The fluorescence lifetime of ANS bound to the enzyme in 0.1 *M* NaCl, 50 m*M* Tris-Cl, and 5 m*M* $CaCl_2$ (pH 8.0), 23°, is 15.2 (±0.2) nsec. In this measurement the ANS concentration was 95 μM and the enzyme concentration was varied from 11.0 to 28 μM so that most of the bound ANS was at the tight sites (>70%). The fluorescence lifetime data obtained for ANS bound to NBD-Tyr-CF_1 (1.0 mol/mol) required a double exponential deconvolution of the data; the lifetimes obtained were 6.4 (±0.4) and 15.4 (±0.2) nsec. If the shorter lifetime is attributed to the tightly bound ANS, the efficiency of energy transfer is 0.58, in good agreement with the steady-state fluorescence measurements. The polarization of bound ANS is 0.349.

The absorption spectrum of quercetin overlaps the emission spectrum of ϵADP and ϵAMP-PNP bound to the two tight nucleotide sites on CF_1 (Cantley and Hammes, 1975a), permitting resonance energy transfer measurements to be made (Figure 6). The quantum yield of bound

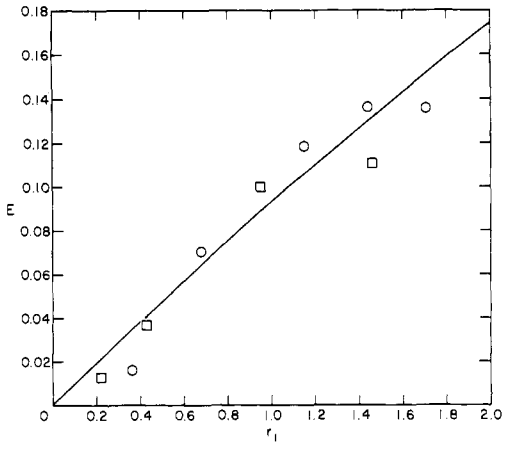

FIGURE 7: A plot of the efficiency of energy transfer, E, from ϵADP (○) or ϵAMP-PNP (□) to quercetin vs. the number of moles of quercetin bound to the "tight" sites per mole of CF_1, r_1. The curve was calculated using eq A3 and the parameters in Table I. The two sets of data gave the same value for R/R_0 using a least-squares analysis.

fluorescent adenine nucleotide analogues, Q_b, at various quercetin concentrations was calculated using eq 8:

$$Q_b = Q_b^0 - [\Delta F/F^0(L_b)][Q_f(L_f) + Q_b^0(L_b)] \qquad (8)$$

where Q_b^0 is the quantum yield of the bound nucleotide in the absence of transfer, Q_f is the quantum yield of the nucleotide free in solution, (L_f) and (L_b) are the free and bound nucleotide concentrations, F^0 is the total fluorescence in the absence of transfer, and ΔF is the change in fluorescence due to transfer. The (L_f) and (L_b) were directly measured as described in the Experimental Section, and Q_f and Q_b^0 were previously determined (Cantley and Hammes, 1975b). (The Q_b^0's were corrected for polarized emission (Shinitzky, 1972).) The results are presented in Figure 7 where the efficiency of energy transfer is plotted as a function of r_1, the number of moles of quercetin bound to the two tight quercetin sites per mole of CF_1. The r_1 were calculated as described above. If the quantum yield of either bound fluorescent nucleotide is plotted against r, the total number of quercetin sites occupied per mole of CF_1, the quenching effect appears to saturate when r equals 2 suggesting that only the tight quercetin sites are involved in transfer. If the efficiency of energy transfer is linearly extrapolated to r_1 equals 2, a value of 0.20 per bound nucleotide is obtained for both nucleotides. For ϵADP, Q_f is 0.59 and Q_b^0 is 0.40, while for ϵAMP-PNP, Q_f is 0.59 and Q_b^0 is 0.47. The number of moles of ϵADP bound per mole of CF_1 in these experiments was 1.40 or 0.78, and the number of moles of ϵAMP-PNP bound per mole of CF_1 was 0.40. The fluorescence of free ϵADP or ϵAMP-PNP, the high absorbance of quercetin, and the large light scattering peak from the protein made determination of the energy transfer efficiency by fluorescence lifetime measurements unreliable in this system.

The quercetin binding experiments were done in the presence of 1 m*M* dithiothreitol to stabilize the quercetin in a reduced state, and it was possible to remove the bound quercetin by passing the enzyme through a Sephadex G-25 column (0.8 cm × 35 cm) equilibrated with 0.1 *M* NaCl, 50 m*M* Tris-Cl, and 5 m*M* $CaCl_2$ (pH 8.0) at 23°. These results indicate that the quercetin is in rapid equilibrium with CF_1. In order to establish the rate of quercetin association with CF_1, both stopped-flow and temperature-jump experi-

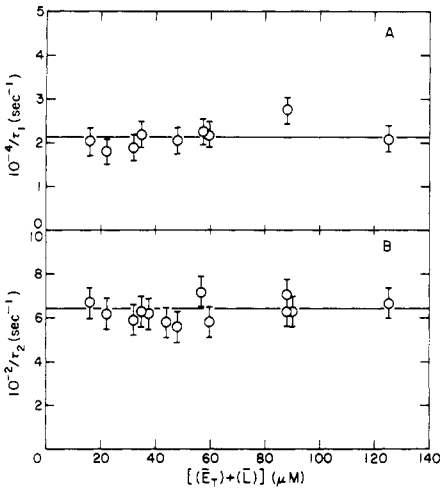

FIGURE 8: (A, B) The reciprocal relaxation times, $1/\tau_1$ and $1/\tau_2$, for the interaction of quercetin with CF_1 as a function of the equilibrium concentrations of tight quercetin sites ($\bar{E}_T$) and free quercetin ($\bar{L}$). Measurements were carried out in 0.1 *M* NaCl, 50 m*M* sodium phosphate, and 1 m*M* dithiothreitol (pH 8.0). The total enzyme concentration varied from 5.2 to 23 μM, and the total quercetin concentration varied from 12.2 to 183.7 μM. The bars represent the experimental uncertainty.

ments were performed. The absorbance change associated with the difference spectrum was completed during the mixing time of the stopped-flow instrument (<5 msec). The temperature-jump technique was used to look for more rapid rate processes in the quercetin-CF_1 interaction. Experiments were performed using both 0.1 *M* NaCl, 50 m*M* Tris-Cl, 5 m*M* $CaCl_2$, and 1 m*M* dithiothreitol (pH 8.0) and 0.1 *M* NaCl, 50 m*M* sodium phosphate, and 1 m*M* dithiothreitol (pH 8.0) with similar results although experiments using the phosphate buffer showed greater relaxation amplitudes. The relaxation process could be resolved into two well-separated relaxation times. The longer relaxation time, τ_2, was calculated from a non-linear least-squares analysis of a single exponential using data after the first relaxation process was essentially complete. In calculating the shorter relaxation time, τ_1, a non-linear least-squares analysis of a double exponential was used with τ_2 held constant at its predetermined value. The resulting relaxation times are plotted in Figure 8A and B as a function of the sum of the equilibrium concentration of tight quercetin sites ($\bar{E}_T$) and free quercetin ($\bar{L}$), as calculated from the total enzyme and quercetin concentration and equilibrium parameters obtained from the binding data. The data indicate that both τ_1 and τ_2 are concentration independent in the concentration range investigated. The average values for τ_1 and τ_2 are 4.7×10^{-5} and 1.56×10^{-3} sec (±10%), respectively.

Discussion

Although the stoichiometry of binding to the tight sites is complicated by the presence of multiple weak sites, the direct and competitive binding measurements involving quercetin and ANS suggest that CF_1 contains two sites which will bind quercetin (K_1 = 19.5 μM, direct binding; K_1 = 34 μM, competitive binding with ANS) and ANS (K_1' = 150 μM) competitively. Since only the tightest binding sites are of interest here, the particular binding model used to correct for binding to other sites is not of great importance; the assumption of two independent sets of binding sites obviously is arbitrary and is by no means unique. The affinity of quercetin and ANS for the tight sites did not appear to be affected appreciably by the NBD-Cl modification of the enzyme. The results obtained indicate that the quercetin-ANS tight binding sites are distinct from the tight nucleotide binding sites and the NBD-Cl reactive site on latent CF_1. Since quercetin completely inhibits the Ca^{2+}-ATPase activity of trypsin-treated CF_1, which contains only the α and β subunits, the quercetin binding sites must be on the two largest subunits of CF_1 (Deters et al., 1975).

The proposal has been advanced that quercetin inhibits enzymatic activities through interaction with protein sulfhydryl or amino groups (Rodney et al., 1950; Carpenedo et al., 1969); however, the results presented here indicate that quercetin is in rapid equilibrium with CF_1 in the presence of 1 m*M* dithiothreitol. The results of stopped-flow and temperature-jump experiments show that the bimolecular association of quercetin and CF_1 is very fast ($\tau < 8 \times 10^{-6}$ sec, the heating time of the temperature-jump apparatus), and is followed by two concentration independent rate processes. The lack of concentration dependence of the relaxation times indicates that conformational changes occur after the initial association reaction and that the enzyme exists predominantly in the initial conformation.[2] It cannot be ascertained whether the conformational changes occur at the tight or loose sites. The inhibitory effect of quercetin may be mediated through these conformational changes.

Before interpreting the energy transfer results, several points are worth considering. First, the probes must be specific for identifiable sites of known specificity; second, the donor fluorescence quenching must be attributed to energy transfer and not to a local environmental change; third, some assessment of the relative orientation of the donor and acceptor dipoles must be made; and finally some model must be assumed to interpret multiple donor and acceptor interactions.

The specificity of the fluorescent ADP and ATP analogues, ϵADP and ϵAMP-PNP, for the tight nucleotide sites and the location of NBD-Tyr on a β subunit of CF_1 were discussed previously (Cantley and Hammes, 1975b). The NBD-Tyr site was shown to be approximately 40 Å away from the tight nucleotide sites and was suggested to be close to the Ca^{2+}-ATPase active site. The energy transfer experiments were designed to select for the tight sites for ANS and quercetin binding, and the specificity of these sites already has been discussed. The occurrence of local donor environmental changes caused by the acceptor cannot be rigorously ruled out. However, the wavelength of the donor fluorescence emission peak is unaltered by the acceptor, as is the affinity of the donor for CF_1. Thus, the fluorescence quenching observed is most likely due to energy transfer.

The efficiency of energy transfer for a given donor-acceptor pair is related to the parameter R_0 defined by eq 9 (Förster, 1959). In eq 9 n is the refractive index of the medium (1.4 for water), Q_D is the quantum yield of the donor, K is an orientation parameter dependent on the relative orientations of the donor emission dipole and the acceptor ex-

[2] This latter conclusion stems from the fact that for a simple ligand binding mechanism such as

$$E + L \rightleftharpoons (EL) \underset{k_{-2}}{\overset{k_2}{\rightleftharpoons}} (EL)'$$

the slow relaxation time, assuming a very rapid bimolecular reaction, is $1/\tau = k_{-2} + k_2/\{1 + K/[(L) + (E)]\}$ where K is the equilibrium constant for the initial step. If τ is essentially independent of concentration and K is not much less than (L) + (E), $k_{-2} \gg k_2$. Similar considerations apply to more complex mechanisms involving a rapid binding step followed by slower conformational transitions.

Table I: Energy Transfer Parameters.

Donor	Acceptor	R_0[a] (Å)	E[b]	R_1[c] (Å)	R_2[c] (Å)	R_3[c] (Å)	R_4[c] (Å)	Method
ϵADP	Quercetin	31.9	0.20[d]	40	34			Fluorescence quenching
			0.18[e]			46	40	Fluorescence quenching
ϵAMP-PNP	Quercetin	32.7	0.20[d]	41	35			Fluorescence quenching
			0.18[e]			48	41	Fluorescence quenching
ANS	NBD-Tyr	31.0	0.55	30				Fluorescence quenching
			0.58	29				Fluorescence lifetime

[a] Assuming $K^2 = 2/3$. [b] Efficiency observed assuming equal quenching of both donors; the approximate uncertainty in the efficiencies is ±10%. [c] R_1–R_4 were calculated from eq A1–A4, respectively. [d] Linear extrapolation to two quercetin molecules bound/enzyme molecule. [e] Extrapolation to two quercetin molecules bound/enzyme molecule according to eq A3.

citation dipole, and J is the spectral overlap integral of donor fluorescence and acceptor absorbance. The overlap integral was calculated according to eq 10 where the summation was taken over 10-nm intervals, $\epsilon_A(\lambda)$ is the extinction coefficient of the acceptor, and $F_D(\lambda)$ is the corrected emission of the donor.

$$R_0 = (9.79 \times 10^3)(JK^2Q_Dn^{-4})^{1/6}\ \text{Å} \qquad (9)$$

$$J = \sum_{\lambda} F_D(\lambda)\epsilon_A(\lambda)\lambda^4\Delta\lambda / \sum_{\lambda} F_D(\lambda)\Delta\lambda \qquad (10)$$

The assignment of a value for the dipole orientation factor, K^2, is difficult (cf. Dale and Eisinger, 1974; Cantley and Hammes, 1975b). For the purpose of calculating R_0 here, K^2 was assigned the value of ⅔ which assumes the donor and acceptor transition dipoles are rotating rapidly in comparison to the donor excited state lifetime (Förster, 1959). The values of R_0 for the donor–acceptor pairs under consideration are given in Table I. The donors, ϵADP and ϵAMP-PNP, have polarizations of 0.33 and 0.25, respectively, when bound to the enzyme (Cantley and Hammes, 1975b) compared with a limiting polarization in a rigid medium of 0.36 (320-nm excitation; Secrist et al., 1972). The bound ANS has a polarization of 0.349 compared with a limiting polarization of 0.396 (Stryer, 1965). The acceptors of energy transfer do not fluoresce sufficiently to allow polarization measurements. The measured polarizations indicate some donor rotation occurs and in view of the relatively long donor excited state lifetimes, it is likely that the acceptor dipoles are also rotating somewhat during this time period. The similar efficiencies measured with ϵADP and ϵAMP-PNP as donors suggest that K^2 is similar for both nucleotides. In any event, large changes in K^2 from the value of ⅔ are required to alter appreciably the distance calculated from energy transfer measurements.

The presence of multiple donor and acceptor sites on the enzyme complicates the interpretation of the efficiency of energy transfer in terms of a distance. The Appendix presents the possible arrangements of two donors and one or two acceptors which allow the extreme values for the donor–acceptor distance, R, along with the relationship for the measured efficiency to R and R_0 for each model. The ANS to NBD-Tyr energy transfer measurements involve two donors and a single acceptor. The efficiencies calculated by steady-state fluorescence (E = 0.55) and by nanosecond lifetime measurements (E = 0.58) are in good agreement indicating that both donors are equally quenched. Thus, eq A1 can be used to calculate this donor–acceptor distance. The energy transfer measurements from ϵADP or ϵAMP-PNP to quercetin involve two donors and two acceptors. Since the energy transfer efficiencies could not be accurately determined by lifetime measurements, it is not possible to determine whether both donors are equally quenched. The equations in the Appendix predict that if both acceptors are involved in energy transfer from a donor, then a plot of the efficiency of transfer vs. the molecules of acceptor bound per enzyme molecule, r, will be nonlinear. The solid line in Figure 7 represents a least-squares fit of the data to eq A3. Individual fits to the ϵADP–quercetin and ϵAMP-PNP–quercetin transfer efficiencies gave virtually identical curves. The variation of the efficiencies with r_1 was also fit to a linear equation, and the saturating efficiency (when r_1 = 2) was used to calculate R from eq A1. Slightly different efficiencies are obtained with the two extrapolation procedures, as given in Table I, but the difference has no appreciable effect on the calculated distances. The uncertainty in the data does not allow distinction between the models of single or multiple acceptors although the curvature of the data suggests multiple acceptors. The distances calculated are summarized in Table I.

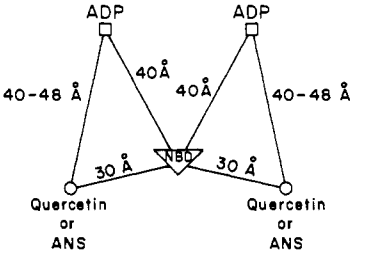

FIGURE 9: A two-dimensional symmetrical representation of the relative positions of ligand sites on solubilized CF_1. The NBD site is located on a β subunit and is proposed as being at or near the active site for ATP hydrolysis.

A plausible symmetrical model for the relationships between the three types of ligand binding sites on CF_1 is presented in Figure 9. The NBD-Tyr is known to be located on the β subunit (Deters et al., 1975), but the specific subunit locations of the two other types of sites remain to be determined.

Appendix: Extreme Possibilities in Multiple Donor and Acceptor Interactions

Chart I illustrates the possible arrangements of two donors and one or two acceptors which allow calculations of the extreme values for the donor–acceptor distance, R. The efficiency measured, E, is calculated assuming equal quenching of both donors. A line drawn between a donor and acceptor indicates energy transfer occurs while if no line is present the acceptor and donor are assumed to be too far apart for energy transfer. Equation A1 is the same as

Chart I

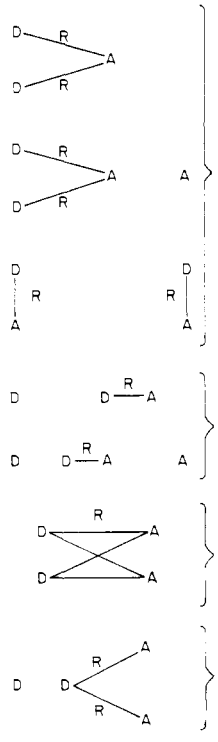

$$E = \frac{(R_0/R)^6}{1 + (R_0/R)^6} \quad (A1)$$

$$E = \frac{(1/2)(R_0/R)^6}{1 + (R_0/R)^6} \quad (A2)$$

$$E = \frac{(R_0/R)^6 (r - r^2/2)}{1 + (R_0/R)^6} + \frac{(R_0/R)^6 (r^2/2)}{1 + 2(R_0/R)^6} \quad (A3)$$

$$E = \frac{(1/2)(R_0/R)^6 (r - r^2/2)}{1 + (R_0/R)^6} + \frac{(R_0/R)^6 (r^2/4)}{1 + 2(R_0/R)^6} \quad (A4)$$

obtained for a single donor–acceptor interaction and assumes only that the donor sites do not interact. Equation A2 assumes that the true efficiency is twice the efficiency measured by steady-state fluorescence quenching since one-half the donor sites do not interact with the acceptor. Equation A3 assumes all donor–acceptor distances are identical. In this equation, r is the number of acceptor sites occupied per enzyme molecule. This equation was calculated assuming a random distribution of acceptors at the acceptor sites as described by Matsumoto and Hammes (1975). Equation A4, like eq A2, assumes the true efficiency is twice the measured efficiency. The efficiencies calculated in eq A1 and A2 from steady-state fluorescence quenching measurements vary linearly with respect to the fraction of acceptor sites occupied.

References

Anderson, D. G., Hammes, G. G., and Walz, F. G., Jr. (1968), *Biochemistry 7,* 1637.

Azumi, T., and McGlynn, S. P. (1962), *J. Chem. Phys. 37,* 2413.

Cantley, L. C., Jr., and Hammes, G. G. (1973), *Biochemistry 12,* 4900.

Cantley, L. C., Jr., and Hammes, G. G. (1975a), *Biochemistry 14,* 2968.

Cantley, L. C., Jr., and Hammes, G. G. (1975b), *Biochemistry 14,* 2976.

Carpenedo, F., Bortignon, C., Bruni, A., and Santi, R. (1969), *Biochem. Pharmacol. 18,* 1495.

Dale, R. E., and Eisinger, J. (1974), *Biopolymers 13,* 1573.

Deters, D. W., Racker, E., Nelson, N., and Nelson, H. (1975), *J. Biol. Chem. 250,* 1041.

Faeder, E. J. (1970), Ph.D. Thesis, Cornell University, Ithaca, N.Y.

Farron, F. (1970), *Biochemistry 9,* 3823.

Förster, T. (1959), *Discuss. Faraday Soc., No. 27,* 7.

Hilborn, D. A. (1972), Ph.D. Thesis, Cornell University, Ithaca, N.Y.

Hilborn, D. A., Harrison, L. W., and Hammes, G. G. (1973), *Comput. Biomed. Res. 6,* 216.

Howell, S. H., and Moudrianakis, E. N. (1967), *Proc. Natl. Acad. Sci. U.S.A. 58,* 1261.

Lang, D. R., and Racker, E. (1974), *Biochim. Biophys. Acta 333,* 180.

Lardy, H. A., Connelly, J. L., and Johnson, D. (1964), *Biochemistry 3,* 1961.

Lien, S., Berzborn, R. J., and Racker, E. (1972), *J. Biol. Chem. 247,* 3520.

Lien, S., and Racker, E. (1971), *Methods Enzymol. 23,* 547.

Matsumoto, S., and Hammes, G. G. (1975), *Biochemistry 14,* 214.

Parker, C. A., and Rees, W. T. (1966), *Analyst 85,* 587.

Rodney, G., Swanson, A. L., Wheeler, L. M., Smith, G. N., and Worrel, C. S. (1950), *J. Biol. Chem. 183,* 739.

Scott, T. G., Spencer, R. D., Leonard, N. J., and Weber, G. (1970), *J. Am. Chem. Soc. 92,* 687.

Secrist, J. A., III, Barrio, J. R., Leonard, N. J., and Weber, G. (1972), *Biochemistry 11,* 3499.

Shinitzky, M. (1972), *J. Chem. Phys. 56,* 5979.

Stryer, L. (1965), *J. Mol. Biol. 13,* 482.